Juxtaparanodal clustering of *Shaker*-like K⁺ channels in myelinated axons depends on Caspr2 and TAG-1

Sebastian Poliak,[1] Daniela Salomon,[1] Hadas Elhanany,[1] Helena Sabanay,[1] Brent Kiernan,[2] Larysa Pevny,[2] Colin L. Stewart,[3] Xiaorong Xu,[4] Shing-Yan Chiu,[5] Peter Shrager,[4] Andrew J.W. Furley,[2] and Elior Peles[1]

[1]Department of Molecular Cell Biology, The Weizmann Institute of Science, Rehovot 76100, Israel
[2]Centre for Developmental Genetics, School of Medicine and Biomedical Science, University of Sheffield, Sheffield S10 2TN, UK
[3]Cancer and Developmental Biology Laboratory, National Cancer Institute at Frederick, Frederick, MD 21702
[4]Department of Neurobiology and Anatomy, University of Rochester Medical Center, Rochester, NY 14642
[5]Department of Physiology, University of Wisconsin School of Medicine, Madison, WI 53706

In myelinated axons, K⁺ channels are concealed under the myelin sheath in the juxtaparanodal region, where they are associated with Caspr2, a member of the neurexin superfamily. Deletion of *Caspr2* in mice by gene targeting revealed that it is required to maintain K⁺ channels at this location. Furthermore, we show that the localization of Caspr2 and clustering of K⁺ channels at the juxtaparanodal region depends on the presence of TAG-1, an immunoglobulin-like cell adhesion molecule that binds Caspr2. These results demonstrate that Caspr2 and TAG-1 form a scaffold that is necessary to maintain K⁺ channels at the juxtaparanodal region, suggesting that axon–glia interactions mediated by these proteins allow myelinating glial cells to organize ion channels in the underlying axonal membrane.

Introduction

Myelinating Schwann cells and oligodendrocytes ensheath the axon in segments separated by the nodes of Ranvier. This arrangement allows saltatory movement of nerve impulses from node to node, and thus, efficient and rapid propagation of action potentials. The nodal region in the underlying axons is organized into several distinct domains, each of which contain a unique set of ion channels, cell adhesion molecules, and cytoplasmic adaptor proteins (Arroyo and Scherer, 2000; Peles and Salzer, 2000). The nodes of Ranvier are bordered by the paranodes, where specialized septate-like junctions are formed between the axon and the myelinating cell (Rosenbluth, 1995). These junctions separate the Na⁺ channels at the nodes from delayed rectifier K⁺ channels located at the juxtaparanodal region beneath the compact myelin at both sides of each internodal interval. The axonal membrane at the juxtaparanodes contains heteromultimers composed of Kv1.1, Kv1.2, and their cytoplasmic Kvβ2 subunit, which may stabilize conduction and help to maintain the internodal resting potential (Wang et al., 1993; Rhodes et al., 1997; Rasband et al., 1998; Zhou et al.,

1998; Vabnick et al., 1999). At the juxtaparanodal region, K⁺ channels colocalize and physically associate with Caspr2, a member of the neurexin superfamily (Poliak et al., 1999). In the peripheral nervous system (PNS), Caspr2 and K⁺ channels are also found along the internodes in two strands that flank a central line of Caspr at the juxtamesaxon and just below the Schmidt-Lanterman incisures (Arroyo et al., 1999, 2001; Poliak et al., 2001). Juxtaparanodal localization of Caspr2 and K⁺ channels in myelinated axons depends on axon–glia interactions and the formation of an axonal barrier that is found at the paranodal junction. Disruption of this junction in several paranodal mutants, including mice deficient for contactin (Boyle et al., 2001), Caspr (Bhat et al., 2001), galactolipids (Dupree et al., 1999; Poliak et al., 2001), and sulfatides (Ishibashi et al., 2002) results in mislocalization of Caspr2 and K⁺ channels to the paranodes.
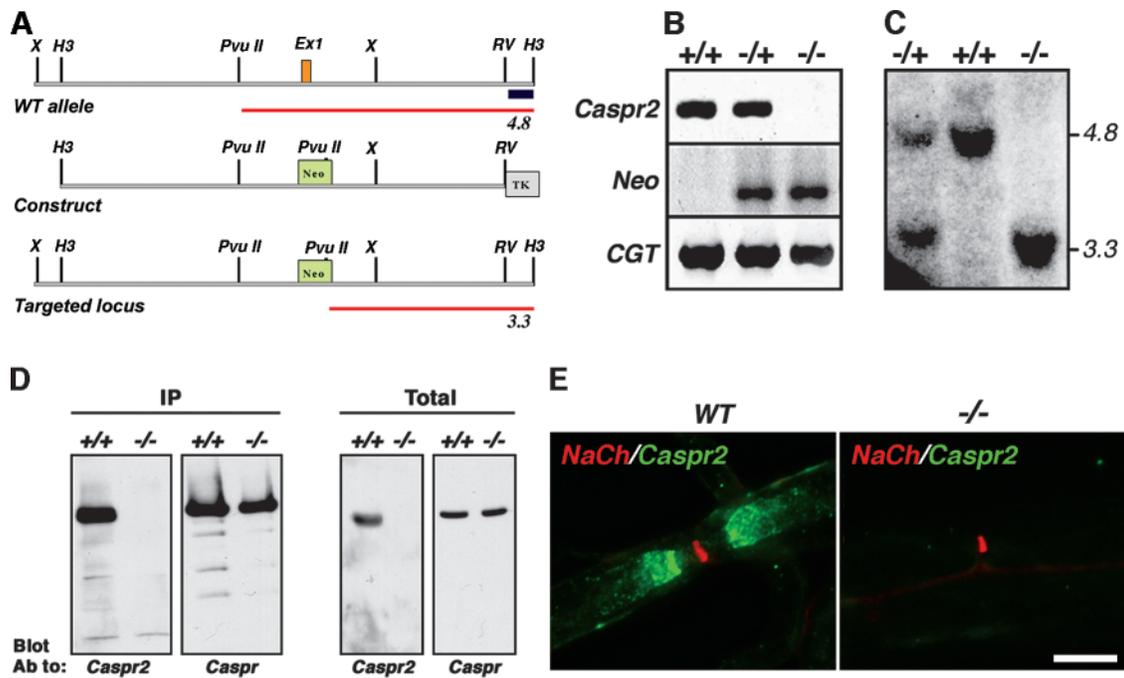
The cytoplasmic domain of Caspr2 contains a short sequence that binds protein 4.1B, as well as a PDZ domain–binding sequence at its COOH-terminal tail (Poliak et al., 1999; Spiegel et al., 2002; Denisenko-Nehrbass et al., 2003). The association of Caspr2 with K⁺ channels is mediated by its COOH-terminal region, most likely through a yet unidentified PDZ-containing protein. The latter have been implicated in the clustering of ion channels and other membrane pro-

Abbreviations used in this paper: 4-AP, 4-aminopyridine; CNS, central nervous system; ES, embryonic stem; PNS, peripheral nervous system.

Figure 1. **Generation of *Caspr2*-null mice.** (A) Schematic map of a genomic DNA fragment containing the first exon of *Caspr2* and flanking region, the targeting construct, and the resulting allele in which exon 1 was replaced by a *neo* gene. The expected size of the DNA fragment detected using the 3′ probe (black box) is labeled in red. (B) Genomic PCR analysis of the indicated animals using specific primer sets of exon 1 of *Caspr2*, *neo*, or a control *CGT* gene as indicated. (C) Southern blot analysis. Genomic DNA digested with HindIII and PvuII was hybridized to the 3′ probe. The expected 4.8-kb and/or 3.3-kb fragments were detected in wild-type (+/+), heterozygote (−/+), and homozygote (−/−) animals. (D) Western blot analysis. Brain lysates prepared from the indicated mice were subjected to immunoprecipitation (IP) and immunoblotting, or directly blotted (Total) using antibodies to Caspr2 or Caspr. (E) Teased sciatic nerves of adult wild-type (WT) or *Caspr2*-null (−/−) mice were double labeled using antibodies to Na+ channel (red) and Caspr2 (green). Bar, 10 μm.

teins within distinct membrane domains (Sheng and Sala, 2001). However, only one such protein (PSD-95) has been found at the juxtaparanodes, and yet this is required neither for the formation of Caspr2/K+ channel complexes, nor for the high density clustering of these molecules at the juxtaparanodal region (Rasband et al., 2002). Based on the close association between Caspr2 and K+ channels, we previously proposed that Caspr2 maintains these channels at the juxtaparanodal region by binding to a ligand present on the glial membrane (Poliak et al., 1999, 2001). Despite the high sequence homology with Caspr, Caspr2 does not interact with contactin, suggesting that it may bind other members of the immunoglobulin superfamily. A likely partner for Caspr2 is TAG-1 (Furley et al., 1990), a GPI-linked cell adhesion molecule closely related to contactin that is expressed by myelinating Schwann cells and oligodendrocytes, and is located at the juxtaparanodes (Traka et al., 2002). To determine whether Caspr2 and TAG-1 play a role in the positioning of K+ channels in myelinated axons, we have generated mice lacking either one of these genes. Here, we show that Caspr2 directly binds to TAG-1 and that both proteins are essential for the clustering of K+ channels at the axonal membrane.

Results

Targeted mutation of *Caspr2* gene in mice

Caspr2-null mice were generated by a standard gene-targeting approach, resulting in the replacement of its first exon,

which includes the translation initiation site and its signal sequence with a *neo* gene (Fig. 1 A). Southern blot and genomic PCR analyses were used to identify the targeted alleles in embryonic stem (ES) cells and subsequently in heterozygous (−/+) and homozygous (−/−) mice (Fig. 1, B and C). Immunoprecipitation and Western blot analyses demonstrated that Caspr2 protein was completely absent in the nervous system of homozygous animals (Fig. 1 D). Similarly, Caspr2 transcript was not detected by RT-PCR performed on homozygous brain RNA (unpublished data). Finally, in marked contrast to the juxtaparanodal appearance of Caspr2 in wild-type and heterozygous animals, no specific signal was obtained when sciatic (Fig. 1 E) or optic nerves (unpublished data) of homozygous mice where immunolabeled with Caspr2 antibodies. These results demonstrate that the animals we have generated are complete *Caspr2* nulls.

Homozygous Caspr2 mutants were born with the expected Mendelian frequency and their appearance was normal. Although generally, *Caspr2*−/− pups were smaller than their heterozygous littermates, this size difference was completely overcome by the second to third month of age (unpublished data). Histological examination revealed no gross abnormalities in the brain of homozygous mice (unpublished data). In contrast to *Caspr*-deficient mice, which display ataxia and tremor and motor deficits (Bhat et al., 2001; unpublished data), *Caspr2* nulls exhibited no signs of neurological abnormalities in their first 20 months of age. Ultrastructural analysis using transmission EM of sciatic
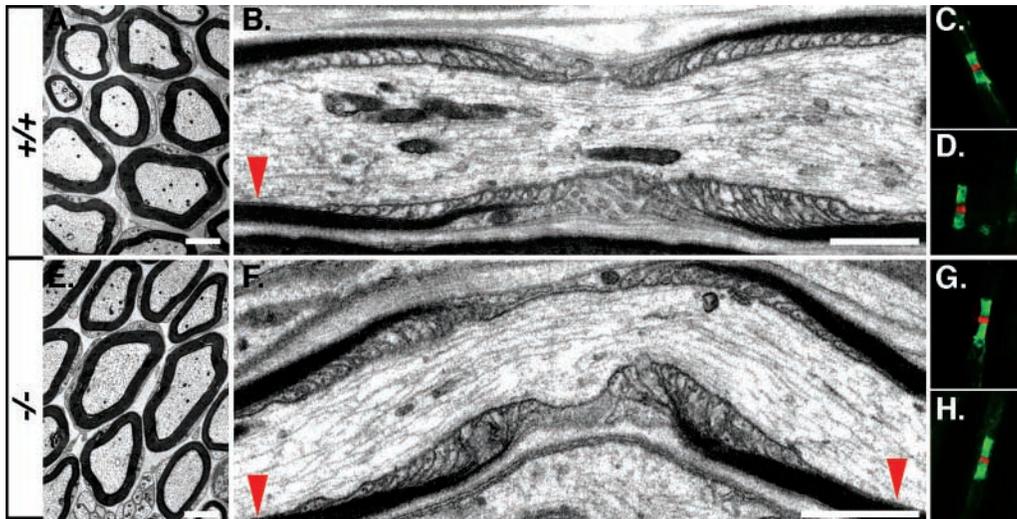
Figure 2. **Morphology of the nodal environs in *Caspr2*−/− mice.** EM pictures of cross (A and E) and longitudinal (B and F) sections of sciatic nerve from adult wild-type (+/+; A and B), or Caspr2-deficient (−/−; E and F) mice are shown. Red arrowheads mark the location of the juxtaparanodes. C, D, G, and H (+/+, C and D; −/−, G and H), show double-immunofluorescence staining of the nodal region using antibodies to Na$^+$ channels (red) and Caspr (green; C and G) or to NF155 (green; D and H). Bars: A and E, 200 nm; B and F, 1 μm.
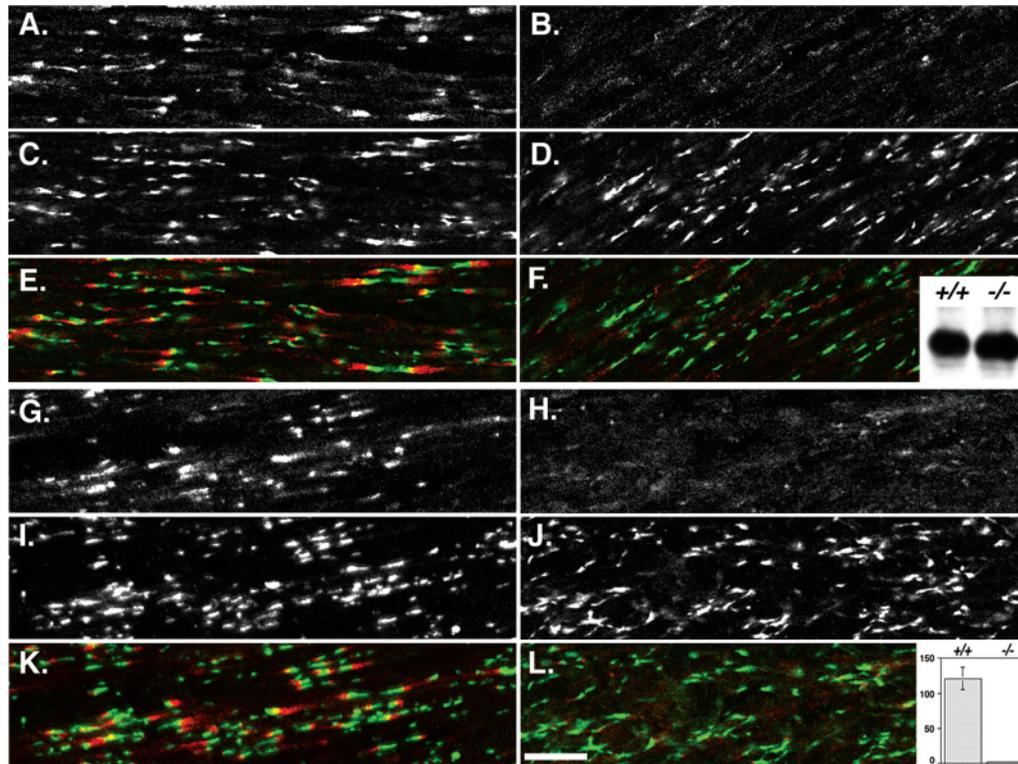
nerves (Fig. 2), as well as optic nerves and spinal cords (unpublished data), showed normal myelin formation and a typical morphology of the nodal environs. The nodes of Ranvier, paranodal septa at the axoglial junction, and the juxtaparanodal region in *Caspr2*−/− were indistinguishable from wild-type animals. In agreement, immunofluorescence labeling using Na$^+$ channels and Caspr or NF155 demonstrated that these proteins were normally localized at the nodes of Ranvier and paranodal junctions, respectively (Fig. 2, G and H). Furthermore, morphometric analysis of optic and sciatic nerves from wild-type and homozygous *Caspr2*−/− mice showed comparable values of axonal caliber, myelin thickness, and G ratios (G ratios: optic nerve, WT 0.79 ± 0.05, KO 0.80 ± 0.05; sciatic nerve: WT, 0.65 ± 0.05, KO 0.65 ± 0.04, $n = 150$/genotype). These analyses indicate that the absence of Caspr2 did not affect myelin formation, axonal ensheathment, or the nodal architecture.

Juxtaparanodal localization of K$^+$ channels is disrupted in nerves lacking Caspr2

Next, we examined whether Caspr2 is required for the correct localization of K$^+$ channels along myelinated axons. Double immunolabeling of optic nerve sections from *Caspr2*−/− mice with antibodies to Caspr and Kv1.2 or Kvβ2 showed that while Caspr was present at the paranodes, these two K$^+$ channel subunits were not concentrated at the juxtaparanodal region as they were in wild-type nerves (Fig. 3). Instead, weak staining of K$^+$ channels was occasionally detected along the internodes, but not in the paranodes, indicating that these channels were redistributed along the internodal region. In agreement, Western blot analysis revealed that optic nerves of wild-type and *Caspr2*−/− mice express similar levels of Kv1.2 (Fig. 3 F, inset). Similar results were obtained using antibodies to Kv1.1 (unpublished data). Occasionally, some weak juxtaparanodal accumulation of K$^+$ channels was observed in 5–10% of the sites. Overall, there was a striking decrease in the fluorescence in-

tensity of juxtaparanodal K$^+$ channels in the mutant (Fig. 3 L, inset; WT 122 ± 28 vs. KO 1 ± 0.6 integrated optical density units), demonstrating that K$^+$ channels were not clustered at the juxtaparanodal region in the central nervous system (CNS). As expected, there was also a significant decrease in the measured total area of K$^+$ channels-labeled juxtaparanodes in these nerves (WT 583 ± 125 μm^2/field of view vs. KO 4.8 ± 2.4 μm^2/field of view). In heterozygous nerves, K$^+$ channels were normally located at this site, although a reduction in the intensity of staining was observed (unpublished data).

Next, we examined the distribution of K$^+$ channels in sciatic nerve of *Caspr2*−/− mice. Double immunofluorescence using antibodies to Caspr and Kv1.2 revealed a similar marked reduction in the accumulation of K$^+$ channels at the juxtaparanodal region in the PNS as observed in the CNS (Fig. 4, A–F). The same results were obtained using antibodies to KV1.1 and Kvβ2 subunits in either frozen sections or teased fiber preparations. Although strong juxtaparanodal accumulation of K$^+$ channels was recorded in 90.3 ± 3.1% of the sites in sciatic nerve sections from wild-type mice, it was only detected in 10.4 ± 6.7% of these sites in the mutant (Fig. 4 I). In most cases, juxtaparanodal labeling of K$^+$ channels in the mutant was detected near the paranodes, which occasionally overlapped with the edge of Caspr staining (Fig. 4 H). In peripheral nerves of wild-type mice, K$^+$ channels flank Caspr in a double strand that apposes the inner mesaxon of the myelin sheath throughout the internodes (the juxtamesaxon; Arroyo et al., 1999; Poliak et al., 2001). In contrast to the reduced accumulation of K$^+$ channels in the juxtaparanodal region, internodal localization of K$^+$ channels appeared normal in the sciatic nerve of *Caspr2*−/− (Fig. 4, H and J), suggesting that different mechanisms control the localization of K$^+$ channels in the juxtaparanodes and along the internodes. Notably, the double juxtamesaxonal lines of K$^+$ channels extended into the juxtaparanodal region and ended as a ring at the border of the paranodes

Figure 3.   **Distribution of K$^+$ channels in the CNS.** Sections of optic nerve from wild-type (A, C, E, G, I, and K) or *Caspr2*-null mice (B, D, F, H, J, and L) were double labeled with antibodies to Caspr (C, D, I, and J) and Kvβ2 (G and H), or Kv1.2 (A and B). Merge images are shown in panels E, F, K, and L. The images were obtained under the same exposure conditions. Note the decrease in K$^+$ channels staining in *Caspr2*−/− nerves. Inset in L shows measurements of the fluorescence intensity labeling of K$^+$ channels in *Caspr2*-null compared with wild-type nerves in integrated optical density units. Three images at 40× were used for each genotype, and errors are given as ± SEM. Inset in F shows the levels of Kv1.2 protein detected by immunoblots in sciatic nerve lysates from wild-type (+/+) or *Caspr2*-null (−/−) mice. Bar, 20 μm.

(Fig. 4, J–L). Western blot of sciatic nerve lysates using an antibody to Kv1.2 (Fig. 4 J, inset), showed that similar amounts of K$^+$ channels are found in *Caspr2* mutant and wild-type nerves, indicating that the reduction of these channels at the juxtaparanodal region resulted from their redistribution along the internodes. Altogether, these results demonstrate that Caspr2 is required for the localization of K$^+$ channels at the juxtaparanodal region in both CNS and PNS myelinated axons.
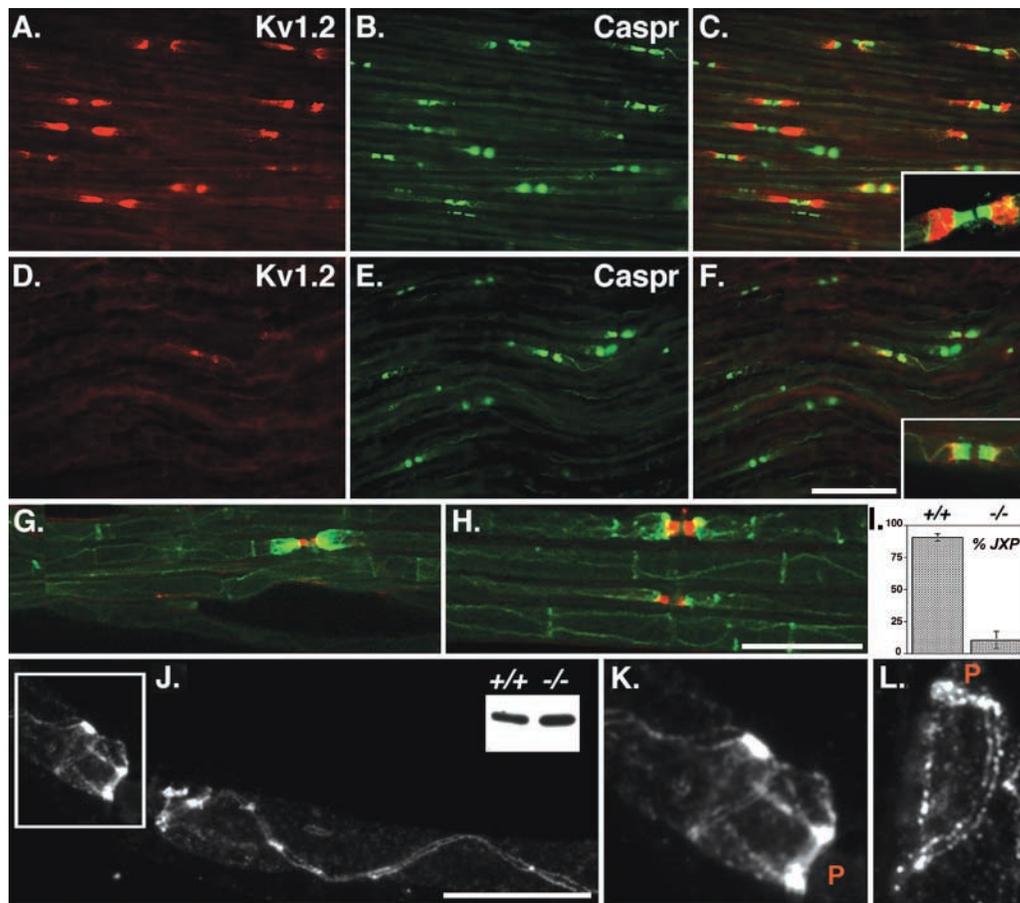
Nerve conduction in *Caspr2*-null mice

K$^+$ channels at the juxtaparanodal region, which are concealed below the compact myelin, were suggested to help in maintaining the internodal resting potential and to prevent aberrant excitation during development (Chiu et al., 1999; Vabnick et al., 1999). To determine whether the reduction in juxtaparanodal K$^+$ channels affected nerve conduction, we recorded compound action potentials of both optic and sciatic nerves from *Caspr2*-null mutants and wild-type littermates. Conduction velocity and refractory period measured in adult or developing nerves at temperatures from 25 to 37°C were not significantly different (P > 0.1) between wild-type and *Caspr2* mutant PNS and CNS (Table I; unpublished data). Furthermore, in sciatic nerve, neither the conduction velocity nor the refractory period were affected by the addition of 1 mM 4-aminopyridine (4-AP), indicating that the remaining K$^+$ channels are still con-

cealed under the myelin as detected by immunolabeling (Fig. 4). It was previously reported that application of 4-AP to wild-type sciatic nerves at 2–3 weeks of age results in repetitive firing (Vabnick et al., 1999). However, we measured conduction in 25 single axons of P13–P20 *Caspr2*−/− sciatic nerves, but saw no evidence for instability (unpublished data). Finally, we examined neuromuscular transmission over the temperature range of 36 to 18°C in P18–23 and 4–5-mo-old *Caspr2*−/− mice. In contrast to mice lacking *Kv1.1*, which exhibit cooling-induced hyperexcitability in the neuromuscular transmission (Zhou et al., 1998, 1999), cooling evoked neither spontaneous activity nor repetitive discharge after a single stimulation in *Caspr2*−/− mice (unpublished data). Based on these series of experiments, we concluded that in spite of the striking

Table I. **Conduction velocities in *Caspr2*−/− optic and sciatic nerves**

Nerve	Temp.	−/−	+/+
Sciatic	25°C	13.0 ± 1.7	11.7 ± 1.7
	37°C	20.8 ± 1.8	21.5 ± 3.0
Optic	25°C	0.95 ± 0.09	0.77 ± 0.1
	37°C	2.10 ± 0.2	2.20 ± 0.3

Recording was done from optic or sciatic nerves of 3-mo-old *Caspr2*-null mutants (−/−) and wild-type (+/+) littermates at the different temperatures as indicated. Conduction velocity is in m/s. Errors are given as ± SEM.

Figure 4. **Reduced juxtaparanodal accumulation of K$^+$ channels in the PNS of *Caspr2*−/− mice.** (A–F) Images showing immunofluorescence staining of sciatic nerve sections from wild-type (A–C) or *Caspr2*-deficient mice (D–F), using antibodies to Kv1.2 (red; A and D) and Caspr (green; B and E) as indicated. Merge images are shown on the right (C and F). Representative images of the nodal region from teased fiber preparations are shown in the insets in C and F. (G and H) Teased sciatic nerves from wild-type (G) and *Caspr2*-null (H) mice, labeled with antibodies to Kv1.2 (green) and Caspr (red). (I) Quantification of the percentage of juxtaparanodes exhibiting normal appearance of Kv1.2, identified as the domain adjacent to Caspr-stained area (n = +/+ 174, −/− 219). (J) Immunolabeling of teased sciatic nerve from *Caspr2*−/− mutant, showing intense staining of Kv1.2 along the internodes, entering the juxtaparanodal region. (Inset) Western blot showing the expression of Kv1.2 in sciatic nerve lysates from wild-type (+/+) and *Caspr2*-null (−/−) mice. (K) Higher magnification of the labeled frame in J. (L) Another example of the localization of K$^+$ channels in the mutant, present in a double line crossing the juxtaparanodal region and terminating as a ring at the border between the juxtaparanodes and paranodes. The location of the paranodes is marked (P) in K and L. Bars: A–H, 20 μm; J–L, 10 μm of the bar shown in J.

reduction in the accumulation of Kv1.1, Kv1.2, and Kvβ2 at the juxtaparanodal region, there was no apparent change in nerve conduction.

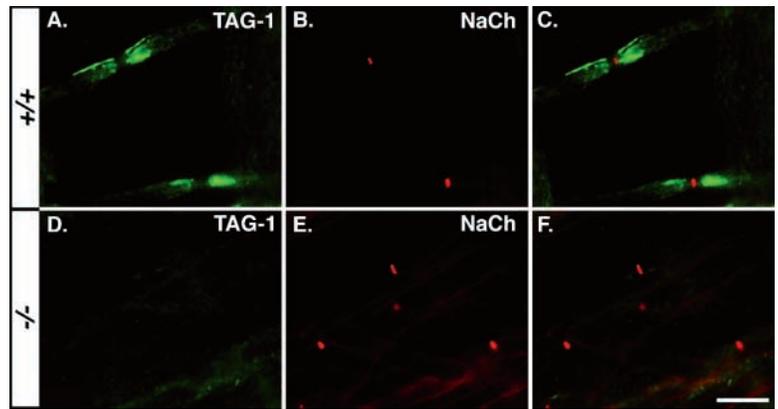## Caspr2-dependent localization of TAG-1 at the juxtaparanodal region

A recent report demonstrated that TAG-1, a GPI-anchored cell adhesion molecule related to contactin, is expressed in Schwann cells and oligodendrocytes and is highly enriched in the juxtaparanodal region (Traka et al., 2002). To investigate the possible involvement of TAG-1 in Caspr2 function, we compared its expression along myelinated nerves in wild-type and *Caspr2*−/− mice. Staining of teased sciatic nerves of wild-type animals using a pAb to TAG-1 and an mAb to Na$^+$ channels confirmed that TAG-1 was concentrated at the juxtaparanodal region (Fig. 5, A–C). In contrast, TAG-1 was barely detected or not detected at all in teased sciatic nerves of *Caspr2*−/− mutant (Fig. 5, D–F). Western blot

analysis revealed that mutant nerves contained lower levels of TAG-1 compared with wild-type animals (unpublished data). Similarly, TAG-1 was absent from the juxtaparanodal region in optic nerve sections of *Caspr2*−/− mutant mice (unpublished data). Thus, we concluded that the accumulation of TAG-1 in the juxtaparanodes depends on the presence of Caspr2 in both PNS and the CNS.

TAG-1 is required for juxtaparanodal clustering of Caspr2 and K$^+$ channels

To determine whether TAG-1 is important for the localization of Caspr2 and K$^+$ channel at the juxtaparanodal region in myelinated axons, we generated *TAG-1*–deficient mice by homologous recombination. These animals were generated by replacing exon 2, which contains the translation initiation site and the signal sequence, and four downstream exons encoding the first two Ig domains, with a tau-LacZ reporter (Fig. 6, A–C). This targeting strategy resulted in the

Figure 5. **Absence of TAG-1 at the juxtaparanode in Caspr2 PNS.** Double-immunofluorescence staining of teased sciatic nerves isolated from wild-type (A–C) or Caspr2-null mice (D–F), using antibodies to TAG-1 (green; A and D) and Na$^+$ channels (red; B and E). Merge images are shown on the right of each row (C and F). Bar, 20 µm.

complete absence of TAG-1 transcript or immunoreactive protein in mice homozygous for the mutant allele (Fig. 6, D–F). *TAG-1* homozygotes appear with the expected Mendelian frequency, are viable, and grow to old age (>14 mo) essentially indistinguishable from their littermates under normal laboratory conditions. Standard histological examination (Nissl) of the central nervous system of these animals revealed no gross morphological abnormalities compared with the wild type (unpublished data), as has also been reported for an independent mutation of the TAG-1 gene (Fukamauchi et al., 2001). Next, we examined the distribution of Caspr2 and Kv1.1, Kv1.2, and their Kvβ2 subunit in sciatic nerves from homozygous and wild-type littermate. As depicted in Fig. 7, although in sciatic nerves from *TAG-1*–null mice Caspr and Na$^+$ channels were properly located at the paranodal junction and the nodes, respectively, Caspr2

was not concentrated at the juxtaparanodal region. In this mutant, weak uniform staining of Caspr2 was detected throughout the internodes, suggesting that in the absence of TAG-1, it was redistributed along the nerve. This conclusion was further supported by immunoblotting analysis, showing that although slightly reduced, Caspr2 was still present in sciatic nerve lysates from *TAG-1−/−* mice (Fig. 7 F, inset). Double-immunofluorescence labeling using an antibody to Caspr and Kv1.2 showed that the concentration of K$^+$ channels at the juxtaparanodes was markedly reduced, very similar to the *Caspr2* homozygotes (Fig. 7, G–L). As in *Caspr2* nulls, Kv1.2 was still present at comparable levels in sciatic nerves of TAG-1 mutant (Fig. 7 L, inset). These results indicate that the localization of Caspr2 and K$^+$ channels in myelinated nerves depends on the presence of TAG-1. Remarkably, in respect to the organization of the nodal envi-
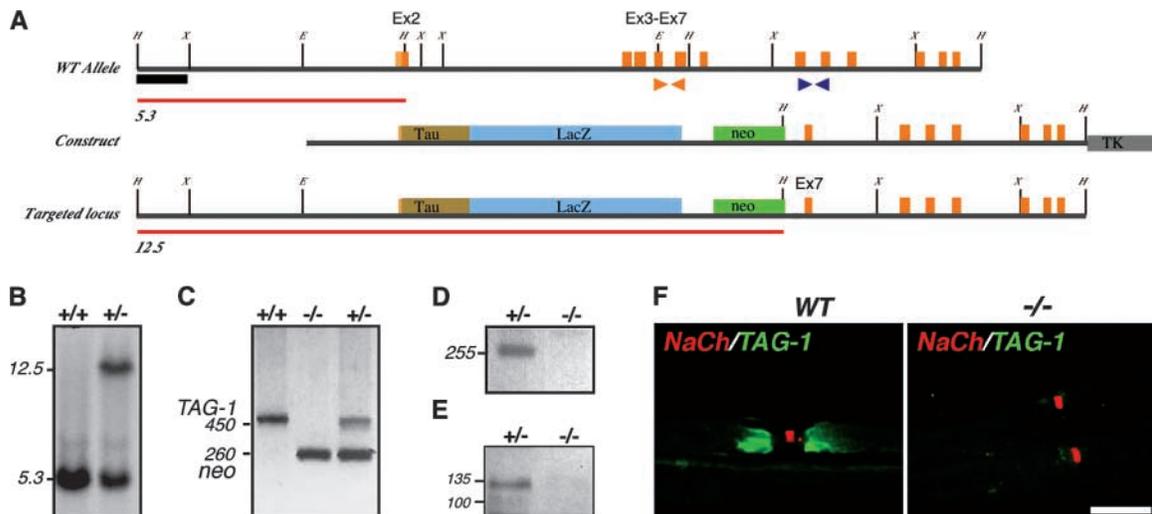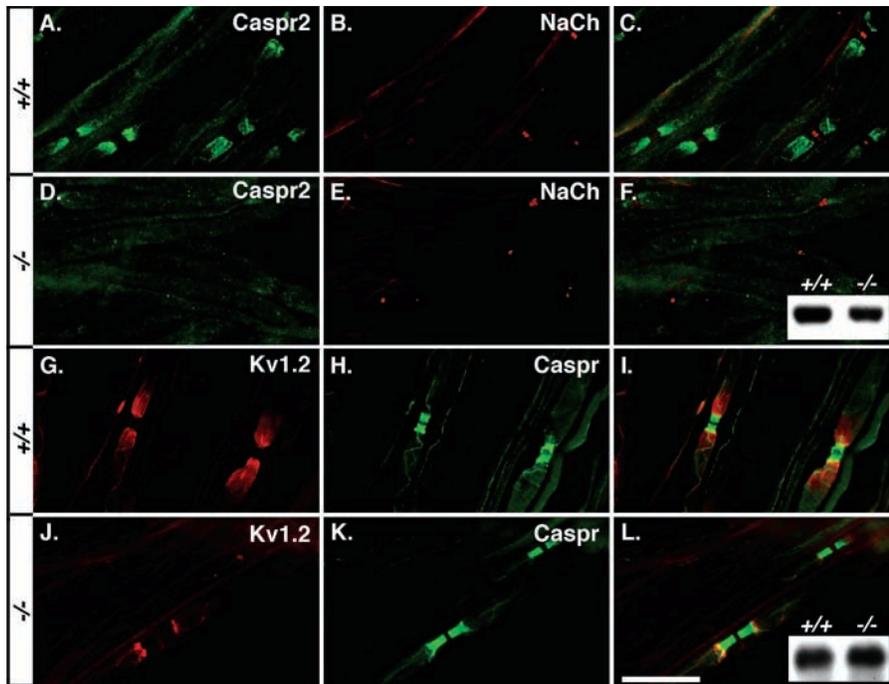

Figure 6. **Generation of *TAG-1*–deficient mice.** (A) Map of recombination strategy showing part of *TAG-1* gene locus including exon 2, which encodes the ATG and signal sequence. Below is the tau-LacZ–containing targeting construct and the predicted locus after targeting. Red lines indicate HindIII fragments detected with 5′ probe (black box). Orange and blue arrows indicate PCR primers used in C and D, respectively. (B) Southern blot showing targeting of construct in ES cells with HindIII digest and 5′ probe. (C) Detection of targeted locus in wild-type (+/+), heterozygous (+/−), and homozygous (−/−) mice by PCR. Wild-type *TAG-1* allele detected by orange primer pair (see A) gives and ~450-bp product, whereas targeted allele detected by neo-specific primers gives an ~260-bp product. (D) RT-PCR to detect TAG-1 mRNA in postnatal cerebellum using blue primer set (see A). The expected 255-bp product is detected in heterozygote but not homozygote animals. (E) Western blot of postnatal cerebellum lysates from heterozygote and homozygote mice blotted with anti-TAG-1 pAbs. TAG-1 protein is detected in heterozygote mice, but not in the mutant. (F) Double-immunofluorescence staining of teased sciatic nerves from adult wild-type (WT), or *TAG-1*–null (−/−) mice using antibodies to Na$^+$ channel (red) and TAG-1 (green). Bar, 10 µm.

Figure 7. **Distribution of Caspr2 and K$^+$ channels in peripheral nerves from TAG-1–deficient mice.** Teased sciatic nerve fibers from wild-type (+/+; A–C and G–I) or homozygous (−/−; D–F and J–L) mice were analyzed. (A–F) Double labeling was performed using antibodies to Caspr2 (A and D; green) and Na$^+$ channels (NaCh; B and E; red). Merge images are shown on the right (C and F). Occasionally, some weak staining of Caspr2 could still be observed at the juxtaparanodes. Western blot showing the expression of Caspr2 in sciatic nerves from wild-type (+/+) and TAG-1–null mice (−/−) is presented in the inset of F. (G–L) Immunofluorescence staining of a similar preparation with antibodies to Kv1.2 (red; G and J) and Caspr (green; H and K). Inset in L depicts the levels of Kv1.2 protein in sciatic nerve lysates from wild-type (+/+) or TAG-1–null (−/−) mice. Bar, 20 μm.

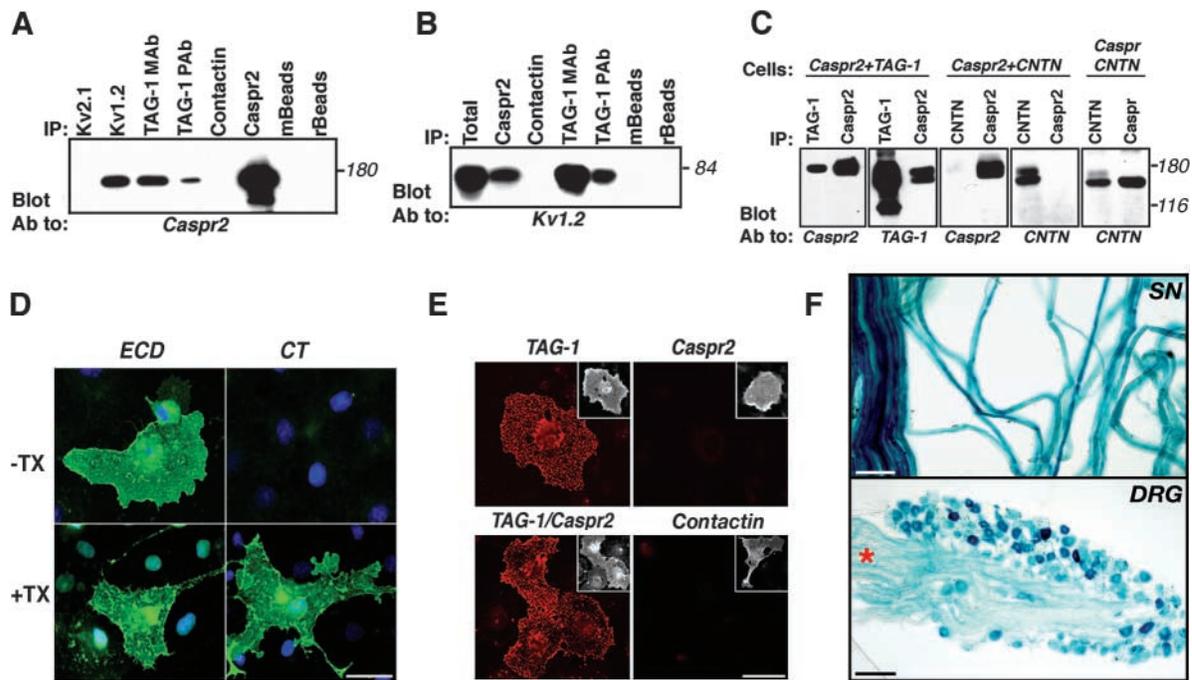rons, it appears that *Caspr2-* and *TAG-1*–null mice are phenotypically identical.

Caspr2 directly interacts with TAG-1

The interdependent localization of Caspr2 and TAG-1 in myelinated nerves, together with the high sequence similarity of TAG-1 with contactin (48% sequence identity), which associates with Caspr (Peles et al., 1997), suggests that Caspr2 and TAG-1 may form a complex at the juxtaparanodal region. This possibility was directly tested using coimmunoprecipitation and binding experiments. As shown in Fig. 8 A, Caspr2 was specifically coimmunoprecipitated from adult rat brain membrane lysates using two different antibodies to TAG-1. In contrast, no association was detected between Caspr2 and contactin. Under the same conditions, Caspr2 was precipitated using an antibody to Kv1.2, but not with Kv2.1, as expected from previous reports (Poliak et al., 1999; Rasband et al., 2002). Furthermore, antibodies to TAG-1 and Caspr2 specifically coprecipitated Kv1.2 from rat brain (Fig. 8 B), suggesting the existence of a tripartite complex of Caspr2, TAG-1, and K$^+$ channels. We estimated that ~5% of Caspr2 molecules are found in association with TAG-1, which is similar to the amount we get with anti-Kv1.2 antibody. Next, we examined the interactions between Caspr2 and TAG-1 in transfected cells. As depicted in Fig. 8 C, TAG-1 antibody precipitated Caspr2 from HEK-293 cells expressing both proteins. Similarly, TAG-1 was detected in Caspr2 immunocomplexes, indicating that these two proteins are associated in these cells. No association between Caspr2 and TAG-1 was observed by mixing detergent lysates of cells independently transfected with Caspr2 and TAG-1, indicating that these proteins interact before cell lysis (unpublished data). In contrast to Caspr, which strongly associated with contactin, no association between Caspr2 and contactin was

detected when coexpressed in HEK-293 cells. As previously reported for Caspr2 (Poliak et al., 1999), we could not detect any interaction between TAG-1 and Kv1.2 in transfected cells (unpublished data), suggesting that the association between TAG-1 and these channels observed in rat brain occurs indirectly, and probably requires Caspr2 and additional unknown adaptor proteins.

Similar to other members of the immunoglobulin superfamily, TAG-1 can interact with itself or with other cell adhesion molecules on the same plasma membrane (i.e., in cis), or on adjacent cells (i.e., in trans; Brummendorf and Lemmon, 2001). Therefore, we set out to examine whether TAG-1 interacts with Caspr2 in trans, using a soluble TAG-1 fused to human IgG (TAG-1–Fc). In contrast to Caspr, which requires contactin in order to exit the ER and reach the plasma membrane (Faivre-Sarrailh et al., 2000), Caspr2 was efficiently expressed on the cell surface of transfected cells in the absence of TAG-1 (Fig. 8 D). As depicted in Fig. 8 E, TAG-1–Fc bound well to cells expressing TAG-1 or TAG-1 and Caspr2, but not to cells expressing Caspr2 alone, contactin, or untransfected cells. Because Caspr2 and TAG-1 are associated when cotransfected (Fig. 8 C), the inability of TAG-1–Fc to bind Caspr2 expressed on the cell surface strongly indicates that these proteins interact in cis.

Although it was demonstrated that TAG-1 is expressed by oligodendrocytes and Schwann cells (Traka et al., 2002), it is still not clear whether it is also found in myelinated axons. To determine whether this is the case, we analyzed the expression of the tau-LacZ gene driven by the TAG-1 promoter in *TAG-1* heterozygous mice (Fig. 6 A and Fig. 8 F). Strong expression was observed in myelinating Schwann cells all over the myelin sheath. In addition, what appeared as axonal staining was detected at the nodes of Ranvier. Furthermore, strong staining was also detected in neuronal cell bodies and processes in adult dorsal root ganglia, demon-

Figure 8. **Association of Caspr2 with TAG-1.** (A) Association of TAG-1 and Caspr2 in rat brain. Immunoprecipitation (IP) from rat brain membrane lysates was performed using antibodies to TAG-1 (IC12; TAG-1 mAb or rabbit pAb; TAG-1 pAb), Kv1.2, Kv2.1, contactin, or Caspr2 as indicated, followed by immunoblotting with an antibody to Caspr2. Anti-mouse (mBeads) or protein A (rBeads) beads were used as additional controls. (B) Co-immunoprecipitation of TAG-1 and K$^+$ channels. Rat brain membrane lysates were subjected to immunoprecipitation using the indicated antibodies, followed by blotting with an antibody to Kv1.2. Total protein extract (Total) was used to determine the location of Kv1.2 on the gel. Note that Kv1.2 was detected using two different antibodies to TAG-1. (C) Association of TAG-1 and Caspr2 in transfected cells. Lysates of HEK-293 cells expressing Caspr2 and TAG-1, Caspr2 and contactin (CNTN), or Caspr and contactin (Cells), were used for immunoprecipitation (IP) and immunoblotting using different combinations of antibodies as indicated in each panel. Note that Caspr2 associated with TAG-1, but not with contactin, which interacts with Caspr. (D) Immunofluorescence staining showing surface expression of Caspr2. COS-7 cells expressing Caspr2 were stained using an antibody against its extracellular (ECD) or intracellular (CT) region, with or without permeabilization as indicated (−Tx, without Triton X-100; +Tx, with Triton X-100). Caspr2 immunoreactivity was detected using the ECD, but not CT antibody in nonpermeabilized cells. Bar, 50 μm. (E) TAG-1 binds homophilically, but not to Caspr2. A soluble TAG-1–Fc was allowed to bind COS-7 cells expressing TAG-1, Caspr2, Caspr2 and TAG-1, or contactin as indicated. Bound Fc fusion was detected using Cy3-conjugated anti-human Fc antibody (red). Note that TAG-1–Fc only bound to TAG-1– or TAG-1/Caspr2-expressing cells, but not to cells expressing Caspr2 or contactin. The insets on the top right of each panel show staining for the corresponding transfected proteins. Bar, 50 μm. (F) Top: β-galactosidase staining of adult sciatic nerve (SN) from heterozygous TAG-1–LacZ animals. Bottom: β-galactosidase staining of adult dorsal root ganglion (DRG). Intense lacZ expression was detected in cell bodies and the track (asterisk). Bars: D and E, 50 μm; F (top), 50 μm; F (bottom), 100 μm.

strating that TAG-1 is expressed by both myelinating glia and the neurons they ensheath. Collectively, these results suggest that Caspr2 and TAG-1 form a juxtaparanodal complex, consisting of a glial TAG-1 molecule and an axonal Caspr2/TAG-1 heterodimer.

Discussion

In myelinated axons, Na$^+$ channels are concentrated at the nodes of Ranvier, separated by the paranodal junction from K$^+$ channels that are clustered at the juxtaparanodal region. The localization of K$^+$ channels in these axons is tightly regulated by the formation of compact myelin and axoglial contact, as suggested by their temporal appearance during normal development and remyelination (Rasband et al., 1998; Vabnick et al., 1999), as well as by their distribution in myelin mutants (Wang et al., 1993) or paranodal mutant mice (Dupree et al., 1999; Bhat et al., 2001; Boyle et al., 2001; Poliak et al., 2001; Ishibashi et al., 2002). However, the exact mechanisms by which K$^+$ channels are clustered at

the juxtaparanodal region remain poorly characterized. In this paper, we provide evidence that Caspr2 and TAG-1 play an essential role in the positioning of K$^+$ channels in myelinated axons.

Caspr2 is required for the accumulation of K$^+$ channels at the juxtaparanodes
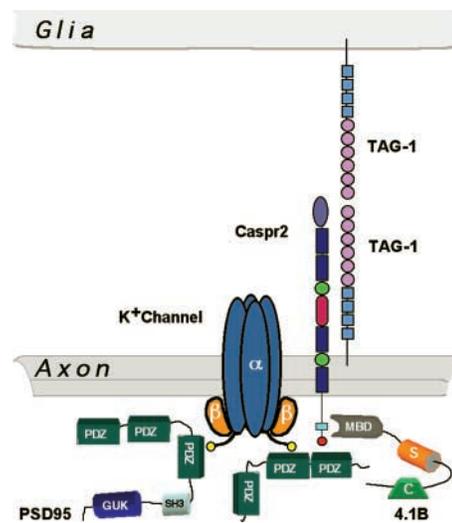
Caspr2 is a member of the neurexin superfamily that colocalizes and associates with Kv1.1, Kv1.2, and their cytoplasmic Kvβ2 subunit at the juxtaparanodal region (Poliak et al., 1999). Caspr2 and K$^+$ channels appear together during development, and their accumulation at the juxtaparanodes depends on the formation of the paranodal junction (Dupree et al., 1999; Bhat et al., 2001; Boyle et al., 2001; Poliak et al., 2001). Here, we showed that targeted disruption of *Caspr2* resulted in a marked reduction in the accumulation of K$^+$ channels at the juxtaparanodes in both PNS and CNS axons. Immunolabeling and immunoblot analyses established that this reduction was not the consequence of their impaired axonal targeting. Instead, in this mutant, K$^+$ chan-

nels were redistributed along the internodal region, indicating that Caspr2 serves as a scaffold that is essential for the accumulation of these channels at the juxtaparanodal region. However, although a similar reduction in the accumulation of K^+ channels at the juxtaparanodal region was also observed in developing nerves (unpublished data), it is currently not clear whether Caspr2 actively participates in the clustering of these channels, or whether it is required for their maintenance at the juxtaparanodal axolemma.

Although both CNS and PNS axons contain a high concentration of K^+ channels and Caspr2 in the juxtaparanodes, the organization of these molecules along the internodal region is quite different (Arroyo et al., 1999, 2001). In the PNS, K^+ channels and Caspr2 are also located as a double line along the internodal region apposing the internal mesaxon and Schmidt-Lanterman incisures (termed the juxtamesaxonal and juxtaincisural line, respectively; Rios et al., 2000; Scherer and Arroyo, 2002). These internodal specializations are a direct continuation of the paranodes and juxtaparanodes and have a similar molecular composition (Tait et al., 2000; Arroyo et al., 2001; Altevogt et al., 2002; Traka et al., 2002), suggesting that they are formed by similar mechanisms. Surprisingly, despite the marked reduction in the juxtaparanodal accumulation of K^+ channels observed in Caspr2- or TAG-1–deficient mice, internodal localization of these channels appeared normal, or even enhanced (Fig. 4, G–H). Hence, it appears that the localization of K^+ channels along myelinated axons is controlled at several levels. First, the clustering of K^+ channels at the juxtaparanodal region depends on the generation of a barrier structure formed at the paranodal junction. In the absence of this junction in mice lacking Caspr (Bhat et al., 2001), contactin (Boyle et al., 2001), CGT (Dupree et al., 1999), or CST (Ishibashi et al., 2002), no barrier is formed, resulting in the movement of K^+ channels toward the nodes. Second, placement of these channels at the juxtaparanodal region requires Caspr2. In contrast to the genetic ablation of *Caspr* (Bhat et al., 2001), which results in accumulation of K^+ channels in the paranodes, deletion of *Caspr2* causes these channels to be redistributed along the internodes. The residual appearance of K^+ channels at the juxtaparanodes in *Caspr2−/−* mice indicates that, although these channels are apparently capable of reaching the juxtaparanode, their localization is not properly maintained. Thus, the present findings suggest that K^+ channels are actively being kept at the juxtaparanode by Caspr2, rather than simply accumulating passively due to their exclusion from the axoglial junction, as has been suggested previously (Rosenbluth, 1976). Finally, a third mechanism that may not require Caspr or Caspr2 seems to regulate the accumulation and maintenance of K^+ channels along the juxtamesaxonal internodal line. This idea is consistent with observations in *Caspr−/−* mice and galactolipid-deficient mice, demonstrating a robust internodal staining of K^+ channels (Bhat et al., 2001; Poliak et al., 2001).

Caspr2 and TAG-1 interactions may mediate axoglial contact at the juxtaparanodes

The localization of Caspr2 at the juxtaparanodes and the clustering of K^+ channels depend on the presence of TAG-1,

Figure 9. **Schematic model describing molecular interactions at the juxtaparanodal region of myelinated axons.** A cis complex of Caspr2 and TAG-1 is present at the axolemma. Homophilic interactions mediate the binding of this complex to glial TAG-1 present on the adaxonal membrane. The association of Caspr2 and K^+ channels involves the PDZ-binding sequence of both proteins, and is likely mediated by yet unidentified PDZ domain–containing protein/s. The juxtaparanodes contain PSD-95, which binds K^+ channels, but not Caspr2. The cytoplasmic region of Caspr2 also binds to protein 4.1B present at this site, which may connect the whole complex to the axonal cytoskeleton. PDZ, PSD-95/discs large/zona occludens 1; GUK, guanylate kinase; SH3, Src homology 3; MBD, membrane-binding domain.

a GPI-anchored cell adhesion molecule from the immunoglobulin superfamily (Furley et al., 1990). We demonstrated that Caspr2 directly associates with TAG-1 in rat brain and that the localization of both proteins at the juxtaparanodes is interdependent, suggesting that the proteins form a scaffold that is essential for the clustering of K^+ channels at this site. In agreement, we found that both Caspr2 and TAG-1 antibodies coimmunoprecipitate Kv1.2 from rat brain. It was previously reported that TAG-1 is expressed by myelinating Schwann cells and oligodendrocytes and is localized at the juxtaparanodes in myelinated nerves (Traka et al., 2002). However, the precise location of this adhesion molecule at the juxtaparanodal region is still unknown. In particular, it is not clear whether it is found only on the glial membrane, the axolemma, or both. Using a tau-lacZ marker under the control of *TAG-1* promoter, we show that in the PNS it is expressed by DRG neurons and their processes, as well as by myelinating Schwann cells. Similarly, in the adult rat spinal cord, TAG-1 was found in motor neurons, as well as in oligodendrocytes (Traka et al., 2002). These results indicate that TAG-1 is expressed by both myelinating glia and the neurons they ensheath. TAG-1 and Caspr2 were associated in transfected cells and a soluble TAG-1–Fc bound to cells expressing TAG-1 or Caspr2/TAG-1, but not to Caspr2 alone, indicating that these molecules are able to form a cis (but not a trans) complex. Thus, our results suggest that these molecules most likely generate a complex consisting of a glial TAG-1 molecule and an axonal Caspr2/TAG-1 heterodimer through homophilic binding of TAG-1 (Fig. 9).

Role of K⁺ channels under the myelin sheath

Despite the dramatic abolishment in juxtaparanodal clustering of Kv1.1/Kv1.2 in *Caspr-2* nulls, there is no change in the excitability of the myelinated nerves. This could be due to the activity of the small amount of K⁺ channels still remaining at the juxtaparanodes (Fig. 4), or to compensation by other K⁺ channels present in these axons (Devaux et al., 2003). In contrast to the clear role of Na⁺ channels in the nodes of Ranvier, the function of the juxtaparanodal K⁺ channels has been more elusive. Two main functions have been proposed for myelin-concealed K⁺ channels (Chiu et al., 1999). First, the internodal K⁺ channels act as a direct current stabilizer to maintain resting potential for the entire nerve (Chiu and Ritchie, 1984). For this function, the spatial localization of K⁺ channels may be less important than the total K⁺ channel content in the internode. Chiu and Ritchie (1984) calculated that if the internodal resting potential is completely abolished, the nodal resting potential would be depolarized by 10–20 mV, enough to have a major impact on nerve excitability. Thus, internodal Kv1.1/Kv1.2 channels could be a major provider of the internodal resting potential. Second, the internodal K⁺ channels may act as an active damper of reentrant excitation (Vabnick et al., 1999). This function is conceptually different from that of providing maintenance of the resting potential, and would require a high spatial clustering of K⁺ channels near the node, consistent with the known juxtaparanodal clustering of Kv1.1/Kv1.2. In *Caspr2* homozygotes, the juxtaparanodal K⁺ channel clustering is abolished, but the total content of these channels remains constant, as does their normal organization along the internodes. The observation that no change in excitability is found in this mutant is thus consistent with a role for myelin-concealed K⁺ channels in maintaining the internodal resting potential.

Role of Caspr family members in ion channel clustering

Caspr2 belongs to a distinct subgroup of the neurexin superfamily, which includes five different proteins in humans (Caspr–Caspr5; Peles et al., 1997; Poliak et al., 1999; Spiegel et al., 2002), as well as neurexin-IV and axotactin in *Drosophila* (Baumgartner et al., 1996; Yuan and Ganetzky, 1999). Of these, three have been implicated in the regulation of ion channel localization. Caspr is essential for the formation of the paranodal junction, and the generation of a membrane barrier that restricts the movement of K⁺ channels from underneath the compact myelin to the node of Ranvier (Bhat et al., 2001). The identification of axotactin in *Drosophila*, a secreted Caspr-like protein produced by glial cells that affects nerve conduction (Yuan and Ganetzky, 1999), suggested that soluble neurexins may also regulate ion channel clustering on the axons, an idea supported by the observation that clustering of Na⁺ channels in mammals during the early phase of CNS myelination is regulated by a soluble factor secreted by oligodendrocytes (Kaplan et al., 2001). By contrast, Caspr2 may function as a scaffold that is essential for retaining K⁺ channels at the juxtaparanodal region. This is reminiscent of the way in which ion channels and neuropeptide receptors are assembled and maintained in synaptic cell–cell contacts (Sheng and Pak, 2000). Hence, it appears that members of the Caspr family and their associated cell adhesion molecules play an important role in the precise organization of myelinated axons through distinct mechanisms. These mechanisms feature different ways by which glial cells control the localization of ion channels in the axonal membrane, thereby facilitating saltatory conduction.

Materials and methods

Derivation of mutant mice

Caspr2. The targeting construct was designed to replace the first exon encoding the ATG and the signal sequence of *Caspr2* with an oppositely directed *neo* gene (Fig. 1 A). The construct was prepared from a 129SvJ genomic phage library. Genomic fragments of 3.5 and 2.0 kb located upstream and downstream of exon 1, respectively, were cloned into the pOSDUPDEL-1 vector (a gift from Oliver Smithies, University of North Carolina, Chapel Hill, NC). This strategy resulted in a deletion of 1,468 bp, including the first exon, as well as a 665-bp (5′) and 697-bp (3′) overlapping sequence. R1 ES cells were transfected with the linearized targeting construct, and recombinant ES clones were selected with G418 and gancyclovir. Clones exhibiting correctly targeted integrations were identified by Southern hybridization, using a 680-bp EcoRV-HindIII fragment genomic sequence not included in the targeting vector (Fig. 1 A) on HindIII/PvuII-digested genomic DNA. Correctly targeted ES cell lines were used to produce chimeric mice by aggregation. Chimeric mice were mated with ICR females, and germ-line transmission was detected by coat color and Southern analysis of tail DNA. Genotyping of progenies was performed by PCR of genomic DNA using primer sets derived from the deletion in Caspr2-targeted allele (5′-TGCTGCTGCCAGCCCAGGAACTGG-3′ to 5′-TCAGAGTTGATACCCGAGCGCC-3′), as well as by using primers for the *neo* or *CGT* genes as described previously (Coetzee et al., 1999). Mice carrying the mutant allele were kept on an ICR (Harlan) background. All experiments were performed in compliance with the relevant laws and institutional guidelines and were approved by the Weizmann's Institutional Animal Care and Use Committee.

TAG-1. The targeting construct consisted of a 1.8-kb EcoRI-NcoI fragment derived from the TAG-1 locus immediately 5′ to, and including part of exon 2, (the first coding exon) up to the ATG start transcription site (an upstream NcoI site was previously deleted by PCR mutagenesis) that was ligated in frame to an NcoI-XbaI fragment containing tau-LacZ (a gift of Peter Mombaerts, The Rockefeller University, New York, NY), an XbaI-ApaI fragment containing a PGK-neopA cassette, a 5.5-kb ApaI-HindIII TAG-1 genomic fragment containing exons 7–13, and a HindIII-SalI fragment containing PGK-tkpA cassette. The linearized vector was introduced into W9.5 ES cells by electroporation, and neo-resistant cells were selected in G418 and screened for homologous recombination by Southern blot using a 1-kb HindIII-XbaI TAG-1 genomic fragment to probe HindIII digested genomic DNA. Homologous recombination was further verified using a 1.2 kb HindIII-HindIII genomic fragment 3′ of the targeted locus on SmaI-digested genomic DNA. Deletion of the targeted sequences was confirmed using a 5′ primer in exon 5 (5′-GGAGGAGAGAGAGACCCCGTGAAA-3′) with a 3′ primer in exon 6 (5′-ACACGAAGTGACGCCCATCCGT-3′) for PCR. Subsequent genotyping used these primers together with primers specific either for neo or for LacZ. Lysates from postnatal cerebellum were separated on 7.5% acrylamide gels by PAGE, blotted to nitrocellulose by routine procedures, and probed with an anti-TAG-1 rabbit pAb (Dodd et al., 1988). RT-PCR was performed on RNA isolated from post-natal cerebellum according to manufacturer's supplied protocols (Hybaid) using primers to exons downstream of the targeted region (5′ primer in exon 8, 5′-CACAGCAGAGCCCACCCTG-3′, 3′ primer in exon 9, 5′-CTGGGAGGCCAGAGGTTC-3′). Mice carrying the mutant allele were backcrossed for 10 generations onto 129SvEv (Mill Hill) before being included in the current analysis. Mice were generated with appropriate UK Home Office and Local Ethical Committee approval.

Antibodies

Antibodies against Caspr, Caspr2 (Poliak et al., 1999), Neurofascin (Poliak et al., 2001), Na⁺ channels, Kv1.2, Kv1.1, Kvβ2 and Kv2.1 (Bekele-Arcuri et al., 1996; Rasband et al., 1999), and anti Contactin (Rios et al., 2000) have been described previously. A mouse pAb against the extracellular region of Caspr2 was raised by immunizing mice with a fusion protein consisting of human IgG1 Fc region and residues 1–1085 of human Caspr2. Rabbit polyclonal and monoclonal IC12 against TAG-1 have been described previously (Dodd et al., 1988).

Immunofluorescence and binding experiments

Preparation and staining of sciatic or optic nerves was described previously (Poliak et al., 1999, 2001). Immunofluorescence was viewed and analyzed using a confocal microscope (Bio-Rad Laboratories) or a microscope (Eclipse E600; Nikon) equipped with a cooled CCD camera (SPOT-II; Diagnostic Instruments). The Image-Pro Plus program (Media Cybernetics) was used to measure the intensity and the area of Kv1.2 juxtaparanodal staining from three random images from each genotype obtained under the same exposure conditions. To define the juxtaparanodes in an image from wild-type nerve, the range of colors was set between 50 and 189. Applying the same conditions to all the images analyzed, the sum of the area or of the integrated optical density, which represents the average intensity/density of each object (juxtaparanode) within the range, was obtained. Fc fusion–binding experiments were done essentially as described previously (Gollan et al., 2002).

Immunoprecipitation and immunoblot analysis

Brain membrane preparation, immunoprecipitation, and immunoblot analysis were done as described previously (Poliak et al., 1999). For comparison of protein levels, three pairs of sciatic nerves of each genotype were dissected, desheathed on ice-cold PBS, cut into 2–3-mm pieces, collected into eppendorf tubes, and frozen in liquid nitrogen. The nerves were then crushed in 150 μl of 25 mM Tris, pH 8.0, and 1 mM EDTA 2% SDS, boiled for 15 min, and spun for 15 min at 15°C. The protein concentration in the supernatant was measured using the BCA protein assay reagent (Pierce Chemical Co.). Immunoprecipitation of brain lysates was done from samples containing 1.2 mg protein each. COS cells were transfected with LipofectAMINE™ reagent (GIBCO BRL) solubilized in SB or SML buffer, centrifuged at 14,000 rpm for 10 min, and the supernatant was used for immunoprecipitation experiments.

EM

Sciatic nerves were fixed for 30 min in situ with freshly prepared 3% PFA, 3% glutaraldehyde, 0.1% picric acid, and 5 mM CaCl$_2$ in 0.1 M buffer cacodylate, pH 7.4. After dissecting out, the nerves were further fixed for additional 60 min, cleaned from surrounded tissue, cut into 1-mm segments, and further incubated in the same fixative for 2 h at 24°C followed by 10 h at 4°C. After extensive washing with 0.1 M cacodylate buffer, the samples were post-fixed with 1% osmium tetraoxide, 0.5% potassium dichromate, and 0.5% potassium hexacyanoferrate in cacodylate buffer and stained en block with 2% aqueous uranyl acetate followed by ethanol dehydration. The samples were then embedded in EMBED 812 (EMS), and sections of 70 nm were cut and stained with 2% uranyl acetate and Reynolds' lead. Samples were examined using a transmission electron microscope (model CM-12; Philips) at accelerating voltage of 120 kV, and were recorded with a 1024 × 1024 pixel CCD camera (BioCam; SiS). Morphometric analyses were done on electron micrographs (2,700×) of sciatic or optic nerves cut in cross sections. Three pairs of 60–70-d-old *Caspr2*−/− or littermate wild-type mice were used for the analysis. Fiber (axon plus myelin sheath) and axon perimeters were measured using the Image-Pro Plus program. Fiber and axon diameters as well as myelin thickness and G-ratio were arithmetically derived. Statistical analysis was done using the InStat program (GraphPad Software, Inc.).

Electrophysiology

Caspr2−/− and +/+ littermate mice were killed by CO$_2$ asphyxiation and sciatic or optic nerves were dissected. In most experiments, sciatic nerves were mechanically desheathed. Nerves were bathed in oxygenated Locke's solution, containing (mM): NaCl 154, KCl 5.6, CaCl$_2$ 2, D-glucose 5, and Hepes 10, pH 7.4. Chamber temperature was maintained with a proportional controller. The ends of the nerves were drawn into suction electrodes for stimulation and recording of compound action potentials. Conduction velocity and refractory period were measured as described previously (Rasband et al., 1998; Vabnick et al., 1999). When used, 4-AP was added to the bath at 1 mM. For muscle recording, isolated phrenic nerve–diaphragm preparations were prepared from wild-type and *Caspr2* mutant mice in two age groups, P18–23 (n = 3 mutants) and 4–5 mo (n = 5 mutants). Compound action potentials were recorded from the muscle surface while the phrenic nerve was stimulated with a bipolar electrode to evoke muscle contraction as described previously using *Kv1.1*-null mutants (Zhou et al., 1998).

References

Altevogt, B.M., K.A. Kleopa, F.R. Postma, S.S. Scherer, and D.L. Paul. 2002. Connexin29 is uniquely distributed within myelinating glial cells of the central and peripheral nervous systems. *J. Neurosci.* 22:6458–6470.

Arroyo, E.J., and S.S. Scherer. 2000. On the molecular architecture of myelinated fibers. *Histochem. Cell Biol.* 113:1–18.

Arroyo, E.J., Y.T. Xu, L. Zhou, A. Messing, E. Peles, S.Y. Chiu, and S.S. Scherer. 1999. Myelinating Schwann cells determine the internodal localization of Kv1.1, Kv1.2, Kvbeta2, and Caspr. *J. Neurocytol.* 28:333–347.

Arroyo, E.J., T. Xu, S. Poliak, M. Watson, E. Peles, and S.S. Scherer. 2001. Internodal specializations of myelinated axons in the central nervous system. *Cell Tissue Res.* 305:53–66.

Baumgartner, S., J.T. Littleton, K. Broadie, M.A. Bhat, R. Harbecke, J.A. Lengyel, R. Chiquet-Ehrismann, A. Prokop, and H.J. Bellen. 1996. A *Drosophila* neurexin is required for septate junction and blood-nerve barrier formation and function. *Cell.* 87:1059–1068.

Bekele-Arcuri, Z., M.F. Matos, L. Manganas, B.W. Strassle, M.M. Monaghan, K.J. Rhodes, and J.S. Trimmer. 1996. Generation and characterization of subtype-specific monoclonal antibodies to K$^+$ channel alpha- and beta-subunit polypeptides. *Neuropharmacology.* 35:851–865.

Bhat, M.A., J.C. Rios, Y. Lu, G.P. Garcia-Fresco, W. Ching, M. St. Martin, J. Li, S. Einheber, M. Chesler, J. Rosenbluth, et al. 2001. Axon-glia interactions and the domain organization of myelinated axons requires neurexin IV/Caspr/Paranodin. *Neuron.* 30:369–383.

Boyle, M.E., E.O. Berglund, K.K. Murai, L. Weber, E. Peles, and B. Ranscht. 2001. Contactin orchestrates assembly of the septate-like junctions at the paranode in myelinated peripheral nerve. *Neuron.* 30:385–397.

Brummendorf, T., and V. Lemmon. 2001. Immunoglobulin superfamily receptors: cis-interactions, intracellular adapters and alternative splicing regulate adhesion. *Curr. Opin. Cell Biol.* 13:611–618.

Chiu, S.Y., and J.M. Ritchie. 1984. On the physiological role of internodal potassium channels and the security of conduction in myelinated nerve fibres. *Proc. R. Soc. Lond. B. Biol. Sci.* 220:415–422.

Chiu, S.Y., L. Zhou, C.L. Zhang, and A. Messing. 1999. Analysis of potassium channel functions in mammalian axons by gene knockouts. *J. Neurocytol.* 28:349–364.

Coetzee, T., K. Suzuki, K.A. Nave, and B. Popko. 1999. Myelination in the absence of galactolipids and proteolipid proteins. *Mol. Cell. Neurosci.* 14:41–51.

Denisenko-Nehrbass, N., K. Oguievetskaia, L. Goutebroze, T. Galvez, H. Yamakawa, O. Ohara, M. Carnaud, and J.A. Girault. 2003. Protein 4.1B associates with both Caspr/paranodin and Caspr2 at paranodes and juxtaparanodes of myelinated fibres. *Eur. J. Neurosci.* 17:411–416.

Devaux, J., G. Alcaraz, J. Grinspan, V. Bennett, R. Joho, M. Crest, and S.S. Scherer. 2003. Kv3.1b is a novel component of CNS nodes. *J. Neurosci.* 23:4509–4518.

Dodd, J., S.B. Morton, D. Karagogeos, M. Yamamoto, and T.M. Jessell. 1988. Spatial regulation of axonal glycoprotein expression on subsets of embryonic spinal neurons. *Neuron.* 1:105–116.

Dupree, J.L., J.A. Girault, and B. Popko. 1999. Axo-glial interactions regulate the localization of axonal paranodal proteins. *J. Cell Biol.* 147:1145–1152.

Faivre-Sarrailh, C., F. Gauthier, N. Denisenko-Nehrbass, A. Le Bivic, G. Rougon, and J.A. Girault. 2000. The glycosylphosphatidyl inositol-anchored adhesion molecule F3/contactin is required for surface transport of paranodin/contactin-associated protein (caspr). *J. Cell Biol.* 149:491–502.

Fukamauchi, F., O. Aihara, Y.J. Wang, K. Akasaka, Y. Takeda, M. Horie, H. Kawano, K. Sudo, M. Asano, K. Watanabe, and Y. Iwakura. 2001. TAG-1-deficient mice have marked elevation of adenosine A1 receptors in the hip-

pocampus. *Biochem. Biophys. Res. Commun.* 281:220–226.

Furley, A.J., S.B. Morton, D. Manalo, D. Karagogeos, J. Dodd, and T.M. Jessell. 1990. The axonal glycoprotein TAG-1 is an immunoglobulin superfamily member with neurite outgrowth promoting activity. *Cell.* 61:157–170.

Gollan, L., H. Sabanay, S. Poliak, E.O. Berglund, B. Ranscht, and E. Peles. 2002. Retention of a cell adhesion complex at the paranodal junction requires the cytoplasmic region of Caspr. *J. Cell Biol.* 157:1247–1256.

Ishibashi, T., J.L. Dupree, K. Ikenaka, Y. Hirahara, K. Honke, E. Peles, B. Popko, K. Suzuki, H. Nishino, and H. Baba. 2002. A myelin galactolipid, sulfatide, is essential for maintenance of ion channels on myelinated axon but not essential for initial cluster formation. *J. Neurosci.* 22:6507–6514.

Kaplan, M.R., M.H. Cho, E.M. Ullian, L.L. Isom, S.R. Levinson, and B.A. Barres. 2001. Differential control of clustering of the sodium channels Na(v)1.2 and Na(v)1.6 at developing CNS nodes of Ranvier. *Neuron.* 30:105–119.

Peles, E., and J.L. Salzer. 2000. Molecular domains of myelinated axons. *Curr. Opin. Neurobiol.* 10:558–565.

Peles, E., M. Nativ, M. Lustig, M. Grumet, J. Schilling, R. Martinez, G.D. Plowman, and J. Schlessinger. 1997. Identification of a novel contactin-associated transmembrane receptor with multiple domains implicated in protein-protein interactions. *EMBO J.* 16:978–988.

Poliak, S., L. Gollan, R. Martinez, A. Custer, S. Einheber, J.L. Salzer, J.S. Trimmer, P. Shrager, and E. Peles. 1999. Caspr2, a new member of the neurexin superfamily, is localized at the juxtaparanodes of myelinated axons and associates with K⁺ channels. *Neuron.* 24:1037–1047.

Poliak, S., L. Gollan, D. Salomon, E.O. Berglund, R. Ohara, B. Ranscht, and E. Peles. 2001. Localization of Caspr2 in myelinated nerves depends on axonglia interactions and the generation of barriers along the axon. *J. Neurosci.* 21:7568–7575.

Rasband, M.N., J.S. Trimmer, T.L. Schwarz, S.R. Levinson, M.H. Ellisman, M. Schachner, and P. Shrager. 1998. Potassium channel distribution, clustering, and function in remyelinating rat axons. *J. Neurosci.* 18:36–47.

Rasband, M.N., E. Peles, J.S. Trimmer, S.R. Levinson, S.E. Lux, and P. Shrager. 1999. Dependence of nodal sodium channel clustering on paranodal axoglial contact in the developing CNS. *J. Neurosci.* 19:7516–7528.

Rasband, M.N., E.W. Park, D. Zhen, M.I. Arbuckle, S. Poliak, E. Peles, S.G. Grant, and J.S. Trimmer. 2002. Clustering of neuronal potassium channels is independent of their interaction with PSD-95. *J. Cell Biol.* 159:663–672.

Rhodes, K.J., B.W. Strassle, M.M. Monaghan, Z. Bekele-Arcuri, M.F. Matos, and J.S. Trimmer. 1997. Association and colocalization of the Kvbeta1 and Kvbeta2 beta-subunits with Kv1 alpha-subunits in mammalian brain K⁺ channel complexes. *J. Neurosci.* 17:8246–8258.

Rios, J.C., C.V. Melendez-Vasquez, S. Einheber, M. Lustig, M. Grumet, J. Hemperly, E. Peles, and J.L. Salzer. 2000. Contactin-associated protein (Caspr) and contactin form a complex that is targeted to the paranodal junctions during myelination. *J. Neurosci.* 20:8354–8364.

Rosenbluth, J. 1976. Intramembranous particle distribution at the node of Ranvier and adjacent axolemma in myelinated axons of the frog brain. *J. Neurocytol.* 5:731–745.

Rosenbluth, J. 1995. Glial membranes and axoglial junctions. *In* Neuroglia. H. Kettenmann and B.R. Ransom, editors. Oxford University Press, New York. 613–633.

Scherer, S.S., and E.J. Arroyo. 2002. Recent progress on the molecular organization of myelinated axons. *J. Peripher. Nerv. Syst.* 7:1–12.

Sheng, M., and D.T. Pak. 2000. Ligand-gated ion channel interactions with cytoskeletal and signaling proteins. *Annu. Rev. Physiol.* 62:755–778.

Sheng, M., and C. Sala. 2001. PDZ domains and the organization of supramolecular complexes. *Annu. Rev. Neurosci.* 24:1–29.

Spiegel, I., D. Salomon, B. Erne, N. Schaeren-Wiemers, and E. Peles. 2002. Caspr3 and caspr4, two novel members of the caspr family are expressed in the nervous system and interact with PDZ domains. *Mol. Cell. Neurosci.* 20: 283–297.

Tait, S., F. Gunn-Moore, J.M. Collinson, J. Huang, C. Lubetzki, L. Pedraza, D.L. Sherman, D.R. Colman, and P.J. Brophy. 2000. An oligodendrocyte cell adhesion molecule at the site of assembly of the paranodal axo-glial junction. *J. Cell Biol.* 150:657–666.

Traka, M., J.L. Dupree, B. Popko, and D. Karagogeos. 2002. The neuronal adhesion protein TAG-1 is expressed by Schwann cells and oligodendrocytes and is localized to the juxtaparanodal region of myelinated fibers. *J. Neurosci.* 22: 3016–3024.

Vabnick, I., J.S. Trimmer, T.L. Schwarz, S.R. Levinson, D. Risal, and P. Shrager. 1999. Dynamic potassium channel distributions during axonal development prevent aberrant firing patterns. *J. Neurosci.* 19:747–758.

Wang, H., D.D. Kunkel, T.M. Martin, P.A. Schwartzkroin, and B.L. Tempel. 1993. Heteromultimeric K⁺ channels in terminal and juxtaparanodal regions of neurons. *Nature.* 365:75–79.

Yuan, L.L., and B. Ganetzky. 1999. A glial-neuronal signaling pathway revealed by mutations in a neurexin-related protein. *Science.* 283:1343–1345.

Zhou, L., C.L. Zhang, A. Messing, and S.Y. Chiu. 1998. Temperature-sensitive neuromuscular transmission in Kv1.1 null mice: role of potassium channels under the myelin sheath in young nerves. *J. Neurosci.* 18:7200–7215.

Zhou, L., A. Messing, and S.Y. Chiu. 1999. Determinants of excitability at transition zones in Kv1.1-deficient myelinated nerves. *J. Neurosci.* 19:5768–5781.